JOURNAL OF GEOPHYSICAL RESEARCH, VOL. 100, NO. C10, PAGES 20,649–20,663, OCTOBER 15, 1995

Offshore wind forcing in the Gulf of Tehuantepec, Mexico: The asymmetric circulation

A. Trasviña

Departamento de Oceanografía Física, Centro de Investigación Científica y de Educación Superior de Ensenada Ensenada, B.C. Mexico

E.D. Barton, J. Brown,[1] and H.S. Velez

School of Ocean Sciences, University of Wales, Menai Bridge, Wales, United Kingdom

P.M. Kosro and R.L. Smith

College of Oceanography, Oregon State University, Corvallis, Oregon

Abstract. Since the early surveys carried out by the Eastern Tropical Pacific (EASTROPIC) and Scripps Tuna Oceanographic Research (STOR) projects in the tropical Pacific off Mexico, the northerly winds which blow over the Gulf of Tehuantepec were described as an important factor controlling the dynamics of this coastal ocean. In January-February 1989 an international team carried out the experiment Tehuano, designed to study the response of the gulf to these wind pulses. The complete evolution of the coastal ocean after an event of moderate intensity was observed. The forcing is characterized by a mostly symmetric, fan-shaped, offshore wind jet, which in turn produces a remarkably asymmetric upper ocean response. While analytical results based on Ekman theory forced by a symmetric offshore wind predict the formation of a symmetric dipolar circulation, the observed flow consists mainly of a large (200 km in diameter) anticyclonic warm-core eddy in the western gulf, with only a weak cyclonic counterpart in the eastern gulf. Intense surface cooling under the wind jet is caused by entrainment of subsurface water into the upper layer. The thermocline in the west deepens with the development of the eddy, which is formed initially by the advection of warm surface waters from west of the gulf. East of the axis of the wind, the mixed layer deepens due to wind-induced entrainment, while, at the same time, shoaling and compression of the deeper isotherms by curl-induced upwelling (Ekman pumping) strengthen the thermocline.

1. Introduction

The occurrence of the northerly winds that blow over the Gulf of Tehuantepec is determined by the topography of the region. The Sierra Madre mountain range, which extends throughout Mexico and Central America with typical elevations of 2000 m, is broken by a 40-km-wide mountain pass with maximum height of 200 m at the Isthmus of Tehuantepec (Figure 1). Cold outbreaks over the North American continent often lead to the establishment of atmospheric high pressure in the Gulf of Mexico, while pressure over the Pacific remains low. The high mountains in Mexico prevent any general passage of cold air farther west and south, except through this gap in the Sierra Madre del Sur, where a fierce cool wind rushes southward over the Gulf of Tehuantepec. West of the gulf, the continental shelf is only about 10 km wide; within and to the east the shelf widens to about 100 km. At the foot of the continental slope is situated a trench 5000 m deep and 50 km wide, while farther offshore, the bottom levels out at slightly more than 4000 m. Thus the area affected by the wind is mostly in deep waters. This wind, known either as a "norte" or "tehuano", extends several hundreds of kilometers out to sea. During the norte season, which lasts from November to February, a series of wind pulses occur, but the conditions for an event may arise at any time of the year. A "typical" event lasts for 3 to 4 days, with speeds of 10 to 20 m s^{-1} and occasionally greater than 25 m s^{-1} [*Stumpf*, 1975].

Although the hydrography of the gulf was not well known before the experiment described here, expeditions undertaken between 1955 and 1960 by the EASTROPIC and STOR projects consistently found a "ridge" or "dome" in a shallow (50 m) and well-defined thermocline, aligned north to south at about 95°W, along the central gulf [*Blackburn*, 1962; *Brandhorst*, 1958] (see also Plate 2a). Both cyclones and anticyclones were detected in the dynamic topography and geomagnetic electrokinetograph (GEK) measurements made after or between wind events. Regions of cool surface water were always linked to these events, but no clear evidence of the thermocline upwelling to the surface was found.

In more recent years, members of the remote sensing community [*Strong et al.*, 1972; *Stumpf*, 1975; *Stumpf and Legeckis*, 1977] characterized the vigorous surface response

[1] Now at Fisheries Laboratories, MAFF, Suffolk, England, United Kingdom.

Paper number 95JC01283.
0148-0227/95/95JC-01283$05.00

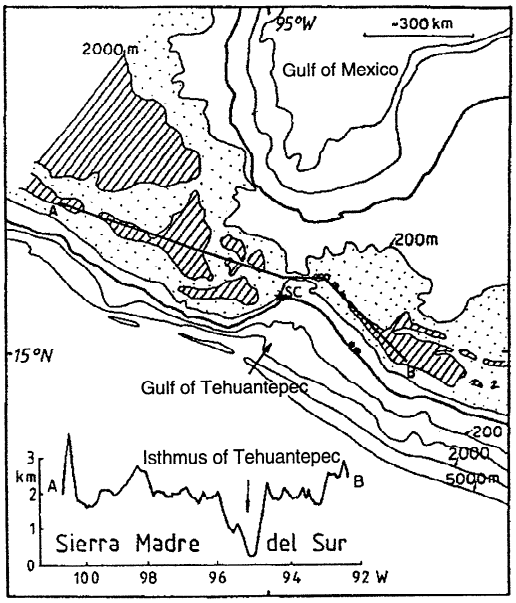

Figure 1. The Gulf of Tehuantepec in southern Mexico. The port of Salina Cruz (SC) is at the head of the gulf and near the Pacific side of the Chivela mountain pass. In the inset, elevations along the Sierra Madre del Sur mountain range show a section of the pass.

by the formation of a wedge-shaped area of cold water emerging from the gulf, extending up to 450 km offshore and followed by the development of a large anticyclonic eddy to the west of the wind axis. The surface cooling was attributed to upwelling, presumably caused by the intensely positive wind stress curl which must be present east of the wind axis.

The propagation of the sea level signal associated with wind events has also been investigated. The studies of *Christensen et al.* [1983] and *Enfield and Allen* [1983)] reveal a strong drop in sea level at the head of the gulf after an event but do not find a northward propagation of the signal. The fall in sea level can be as much as 30 cm, as observed in the negative sea level events in the Salina Cruz record of *Enfield and Allen* [1983].

Analytical solutions to the traditional Ekman problem forced by a symmetric offshore jet [e.g., *Crepon and Richez*, 1982] predict equally strong anticyclonic and cyclonic eddies to the right and left of the wind, caused by negative and positive wind stress curls and the downwelling/upwelling associated with it. Because this feature (vortex symmetry) has not been observed, additional elements in the dynamic balance must be responsible for the inhibition of the cyclonic circulation and the generation of an asymmetric flow pattern.

Attempts have also been made to understand the circulation of the gulf with numerical layered models. *Clarke* [1988] reproduced the shape of the pycnocline with a 1½-layer model forced by an asymmetric wind jet that followed an inertial circle. *McCreary et al.* [1989] were the first to recognize the relevance of nonlinear processes in the dynamics of the phenomenon, namely, the production of an ageostrophic offshore jet, as well as the importance of entrainment processes in producing the observed surface cooling. These authors conclude that entrainment is responsible for the weakening of the cyclonic eddy, whereas advective processes strengthen the circulation around the anticyclonic eddy. They obtain an asymmetric dipolar circulation with a weaker cyclonic eddy and reproduce observed values of the sea level depression at the head of the gulf by forcing a nonlinear 1½-layer model with a symmetric offshore wind. Entrainment from the lower to the upper layer was allowed in order to produce surface cooling and to prevent the interface from surfacing. In agreement with results of *Christensen et al.* [1983] and *Enfield and Allen* [1983], the sea level depression at the coast does not produce a poleward propagating wave.

In the pages that follow, data gathered during the experiment Tehuano of January-February 1989 are used to describe the main asymmetries of the flow. Some remarks about the aforementioned models are included in section 3.

2. Observations

A two-ship survey of the area was carried out before and after a moderately strong wind event which commenced on January 21, 1989. The observations included here come from advanced very high resolution radiometer (AVHRR) satellite imagery, moored thermistor chains, moored and shipboard acoustic Doppler current profilers (ADCP), and current meter moorings, as well as from conventional conductivity-temperature-depth (CTD) casts and towed-undulating CTD (Seasoar) sections (Figure 2). Three thermistor chain moorings were deployed at sites D1, D2 and D3 (Figure 2), all with 11 thermistors spaced every 7.5 m, starting at 4 m nominal depth and with a pressure and temperature logger nominally at 113.4 m; only two were recovered (D2 and D3).

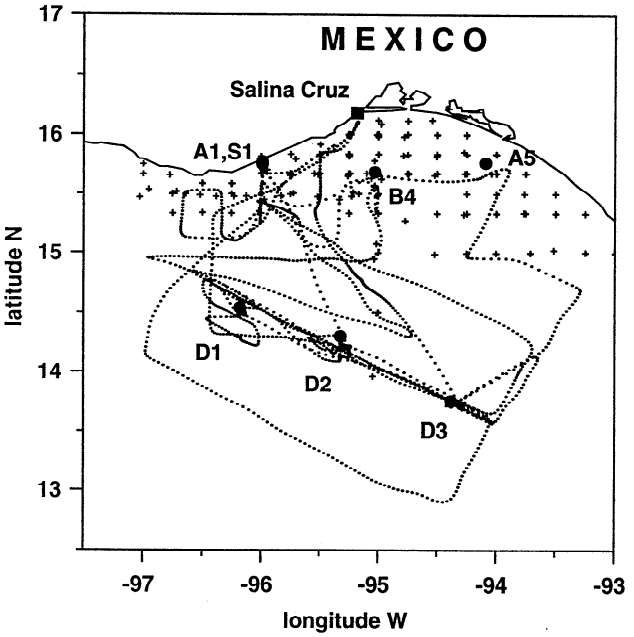

Figure 2. The Tehuano experiment of January-February 1989 cruise track and mooring positions. Small crosses mark the hydrographic stations occupied by the R/V *El Puma* near the coast. The dotted line follows the track of the R/V *Wecoma*. Positions S1, A1, B4, and A5 indicate current meter moorings deployed over the shelf. Positions D1, D2, and D3 indicate the deep mooring sites, where thermistor chains and upward looking acoustic Doppler current profilers (ADCPs) were deployed.

The chain at the central site (D2) provided data for the period between January 17 and 27, and at the eastern mooring (D3), data were recorded for the period January 20 to February 6. Here no pressure record was obtained, and so corrections to the nominal depths for the oscillation of the chain could not be applied. However, the estimated uncertainty in the depth of the thermistors does not exceed 9% of their nominal depths and is estimated to have been less than 6% most of the time. Self-contained 150-kHz ADCPs were deployed adjacent to the thermistor chain sites (D1, D2, and D3), looking upward from approximately 130 m depth and sampling the currents in 4-m cells (bins). Current meter moorings were installed over the shelf (designated S1, A1, B4, and A5 in Figure 2) with Aanderaa RCM7 (at S1) and Niskin-type General Oceanic (at all other moorings) current meters. An overview of the experiment is given by *Barton et al.* [1993].

2.1. Forcing and Asymmetric Flow

Winter nortes are commonplace for the inhabitants of the coast of the Gulf of Tehuantepec; the region is constantly being blown by northerly winds of diverse magnitude and duration. Weak events do not greatly affect the mesoscale circulation but help maintain low-surface temperatures along the central gulf, relatively close to shore. At least one event with average wind speeds greater than 10 m s^{-1} took place before the start of the survey. This occurred from January 16 to 18, when the northerly winds reached 12 m s^{-1}. Several northerly blows took place during the period of measurements, but the event of January 21 was the most intense (Figure 3).

The time evolution of the event of January 21 is given by an estimate of the wind speed in the central gulf (Figure 3), as calculated from the near-surface backscatter signal of the central ADCP mooring D2. *Brown et al.* [1992] showed this signal to be an accurate predictor of winds observed both on board ship and at the moorings. The wind direction at D2 varied little from northerly according to the available observations from the ship. During the onset of the norte the wind accelerated from about 2 to 12 m s^{-1} in less than 3 hours and reached a maximum of 14 m s^{-1} 12 hours later. It decreased gradually over the next 48 hours to around 9 m s^{-1} and fell in two abrupt steps to almost complete calm late on January 24.

Although the shape of the forcing is not completely revealed by the observations, shipboard wind data from the two research vessels were presented in a previous paper to show that the wind spreads out quite symmetrically with increasing distance from the head of the gulf [*Barton et al.*, 1993] (Plate 1a). The satellite image of January 21 (Plate 1a) shows the surface temperature field after the onset of the event and has superimposed on it the composite of all shipboard wind measurements carried out during the experiment. These observations were gathered over 3 weeks by two different ships, and each value represents the area average for a 0.1° square grid. North of 14°N, in the eddy generation area, the wind appears quite symmetrical about its north-south axis. Although it does appear to curve anticyclonically farther offshore, its degree of curvature is not significant when compared with its lateral spread, and the wind can be approximated as having a north-south direction near the coast, where the eddy is generated.

An intense thermal anomaly identifies the area stirred by the wind (Plate 1a). This anomaly reaches some 400 km offshore, describing a comma-shaped strip 200 km wide at the center of the gulf. The coldest water of 16°C, found at the center rather than at the head of the gulf, contrasts with the warm (25°C) surrounding waters. The axis of the anomaly extends from the head of the gulf southward, roughly along 95°W, where the wind blows strongest. Currents measured by both shipboard and moored instruments indicated strong accelerations as soon as the wind jet was established. The cusplike features north of 14°N on the western flank of the cold anomaly on January 21 (Plate 1a) were seen in later

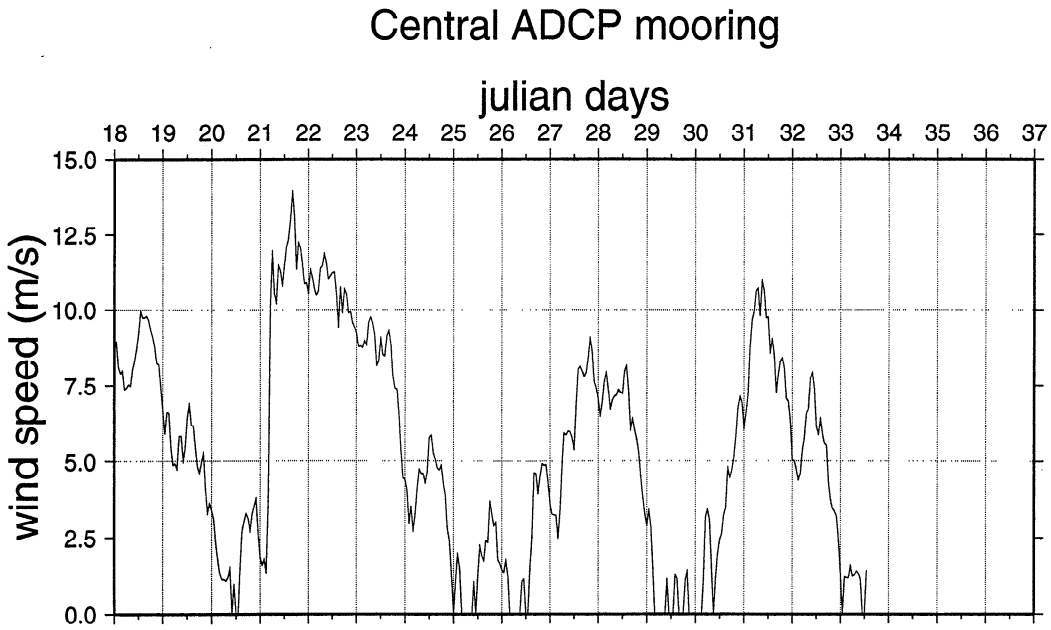

Figure 3. Wind speed at the central mooring (D2) estimated from the automatic gain control (AGC) of an upward looking ADCP [*Brown et al.*, 1992].

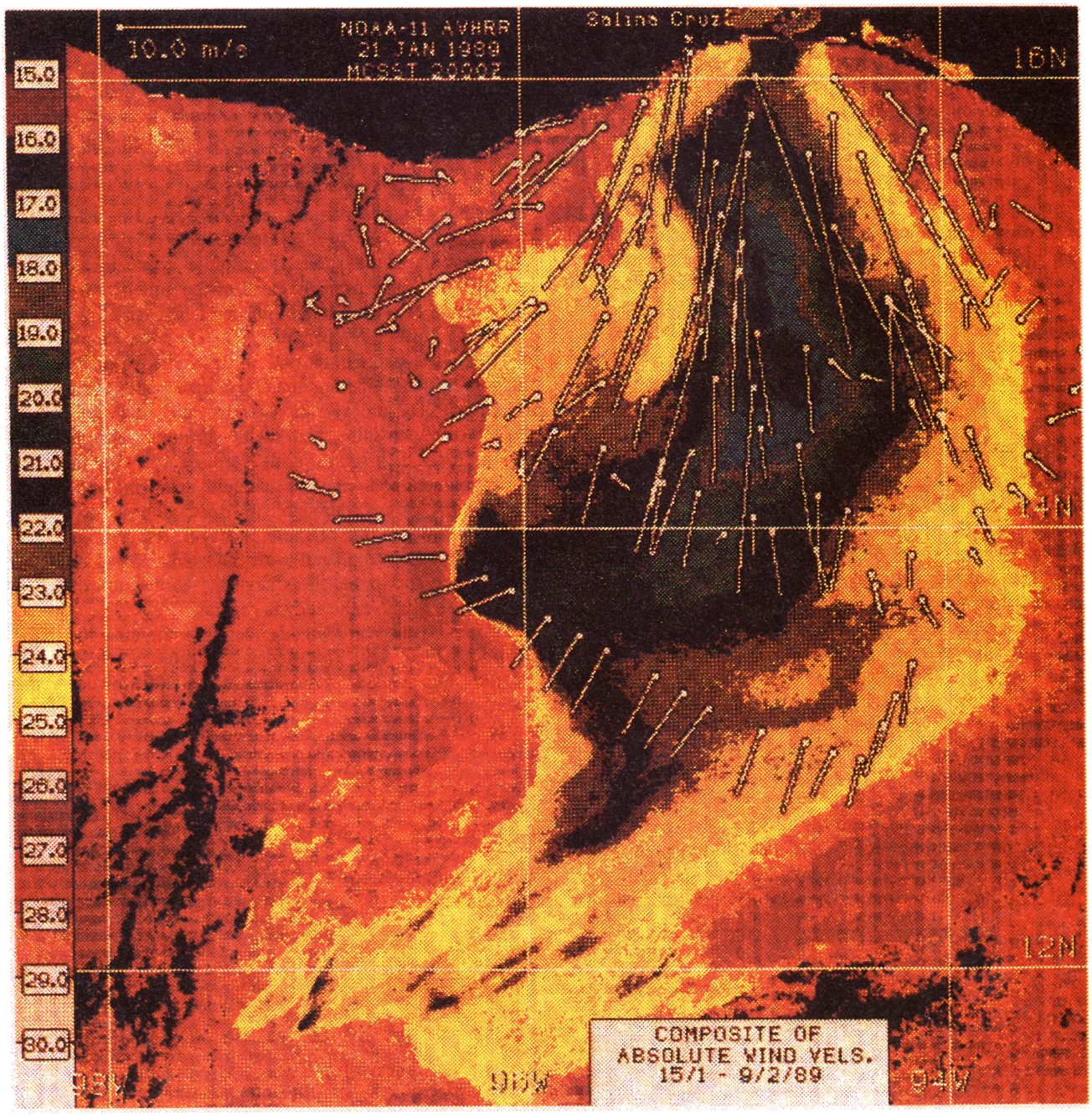

a

Plate 1. Satellite images during and after the wind event. The color scale indicates sea surface temperature (SST) from AVHRR. (a) The wind event of January 21, showing SST plus composite of all shipboard wind measurements. (b) The state of the Gulf of Tehuantepec on January 30, showing SST plus composite of all shipboard ADCP current measurements between January 24 and February 2.

images to merge together during the days subsequent to the wind event, forming the single, large anticyclonic feature evident on January 30 (Plate 1b). Prior to January 21, shipboard ADCP measurements reveal a weak anticyclonic circulation in the eddy generation area. The shape of the thermocline in the western gulf before the event (Plate 2a) is also consistent with the presence of a weak anticyclonic circulation produced by previous wind events and enhanced by the event of January 21. The southward extension of cool surface water (Plate 1a) delineates the eastern flank of an eddy formed near the coast by a previous event, now found farther offshore. The faint outline of this and other offshore eddies can be seen intermittently throughout the imagery gathered for this experiment, as well as in historical images of the area [*Stumpf and Legeckis*, 1977, *Leben et al.*, 1990], consistent with their westward displacement after being generated near the coast.

Superimposed onto the image of January 30 (Plate 1b) are all the shipboard ADCP data gathered between January 24 and February 2. A second wind event took place between January 26 and 29 (Figure 3), but it was significantly weaker than the first (maximum wind speed averaged 7.5 m s^{-1}). Its

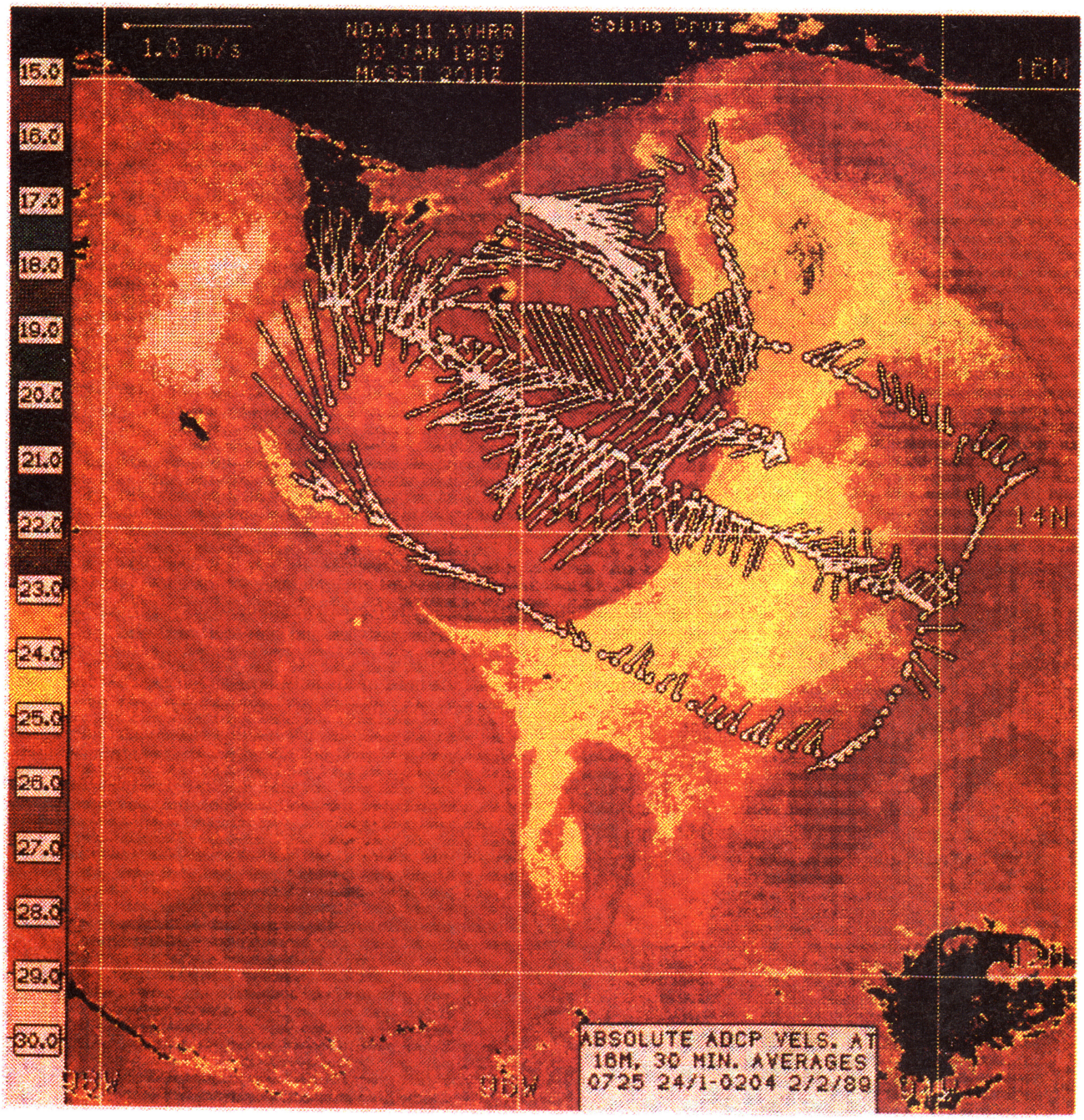

b

Plate 1. (continued)

occurrence does not alter the existing surface temperature patterns, as seen in the imagery, or the surface currents found in the ADCP or current meter data. It probably intensified the existing coastal circulation, but no observations are available there at that time. Even though the current observations are not synoptic, the apparent persistence of the flow regime over a period of almost a week indicates a remarkably consistent pattern of circulation. The main feature is the fully developed anticyclonic eddy occupying all the western gulf. The axis of the offshore current now follows the curvature of the eddy, with maximum speeds in excess of 1 m s^{-1}. The whole nearshore region is now characterized by warm water of approximately the same temperature (27°C), as the surface temperature anomaly has warmed following cessation of the strong wind. In the eastern gulf the current vectors show a weak cyclonic circulation around 14°N, 94.8°W. *Barton et al.* [1993, Figure 3] find a strong correspondence between these current measurements and the dynamic topography, and they show a sea surface elevation associated with the eddy, while the area of the cyclonic circulation coincides with a depression of the sea surface.

2.2. Currents

2.2.1. Overview. An overall view of the horizontal current regime is provided by the progressive vector diagrams (PVDs)

of three near-surface current meters distributed over the shelf and three upward looking ADCPs moored offshore across the Gulf of Tehuantepec (Figure 4). All the current observations were made in the upper layer above the thermocline (40 m). Each PVD starts where the mooring label is drawn and circles along the trajectories mark the end of 24-hour periods. Each PVD starts at 1100 UT (0500 PST) on January 21 and finishes at 0600 UT (0000 PST) on January 26. The pattern of flow shows a convergence of the coastal currents (at A1 and A5) toward the head of the gulf and an offshore flow along the axis of the wind jet (at B4 and D2). To the eastern side of the wind jet (D3) the flow appears uniformly northeastward, toward shore, while in the west (D1), the flow is strongly westward.

Examining the PVDs in more detail shows that this overall pattern varied strongly during the 5 days. At mooring A1 a coastal flow toward the head of the gulf starts on January 21 and continues for most of the 5-day period. On January 22 the net alongshore flow appears to stop (where the circles for the end of January 21 and 22 are superimposed onto each other) due to local meandering and deceleration of the flow. Inspection of the 5-day image sequence, current meter, and ADCP data around mooring A1 reveals motion of a warm temperature front toward the head of the gulf. These observations are consistent with the presence of a narrow (20 to 40 km) coastal flow past the A1 mooring site. From January 23 to 25 this alongshore flow is still present at A1, but its waters do not reach the head of the gulf. Instead, these waters feed the eastward expansion of a tongue of warm water that extends toward the central gulf, past mooring site B4.

At mooring A5 the current flows toward the head of the gulf during the first hours of the event. On January 22 the flow slows down and rotates clockwise. It is not until January 24, after the end of the event, that the alongshore flow is reestablished.

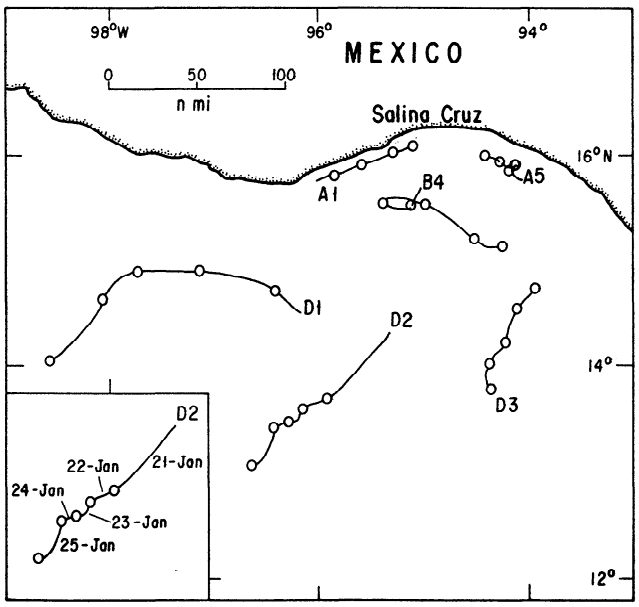

Figure 4. Overview of the horizontal current regime showing progressive vector diagrams (PVDs) of six near-surface current meters and upward looking ADCPs. For clarity the inset shows the dated diagram at mooring D2.

At mooring B4, off the head of the gulf, the flow responds to the event with a moderate (0.2 m s^{-1}) offshore drift during January 21 but on January 22-23 it rotates through 270° anticyclonically. This rotation is produced by the eastward extension of the western coastal current discussed previously. This eastward flow past B4 is consistent with the western coastal current contributing warm surface waters to the developing eddy. During the later part of the period shown the flow formed part of the northeastern limb of the anticyclonic eddy.

At D2, in the central gulf, close to the location of the maximum temperature anomaly, the offshore current was strongest at the peak of the wind event on January 21. It then continued to flow offshore at reduced speed during the following days. At D3, where the flow is in the opposite direction, i.e., northward, the current is modified by an inertial oscillation. At the latitude of 15°N the period of the oscillation is 46 hours.

On the western side of the gulf, the overall cyclonic curvature of the D1 PVD is a result of shifts in position and expansion of the anticyclonic eddy documented by the imagery sequence (not shown). On January 21 and 22, D1 experienced northeastward flow as a result of its location on the southwestern circumference of the eddy, but as the eddy grew by expanding eastward and southward, currents at D1 became more westward and later southwestward.

Summarizing, the onset of the wind starts convergent flows toward the head of the gulf, both at A1 and A5. The coastal flow past A1, instead of reaching the head of the gulf, produces an eastward extension of warm water. This, in turn, produces the eastward flow at B4 that contributes to the formation of the eddy. At A5 the flow decelerates during part of the event, but as the wind weakens, the convergent flow is reasserted. None of the coastal flows reaches the head of the gulf during these 5 days; their thermal signature in the imagery shows that convergence occurs after the eddy is fully formed, which is on January 29. On January 21 the offshore component of flow in the central gulf is weaker near the head of the gulf (around mooring B4) than further offshore (D2). Throughout the event the surface currents in the eastern gulf (D3) persisted toward the north-northeast. Consequently, the waters that form the circulation around the eddy, at least initially, come mainly from the west, outside the gulf.

2.2.2. Time series in the upper layer. The time series of currents from three upward looking ADCPs deployed across the Gulf of Tehuantepec (locations D1, D2, and D3 in Figure 2) are presented in Figure 5 as stick diagrams for the complete period of observations and for depths between 16 and 140 m. Again, the response of the currents at different depths shows large differences across the gulf. Whereas in the central site (Figure 5b) the wind produces a strong offshore (southward to southeastward) flow restricted to the upper 30-40 m during the event, in the western mooring (Figure 5a) the current flows toward the northwest on January 21 and 22 from the surface down to 80 m depth, and then it rotates anticlockwise over the following days. East of the axis of the wind (Figure 5c), the currents show a steady northward to northeastward flow throughout the water column. Inertial oscillations (inertial period of 46 hours at 15°N) between 20 and 30 m depth appeared stronger from January 21 to 25, possibly as a result of the wind pulse.

Toward the end of the period of observations, the currents at the eastern mooring become progressively more coherent

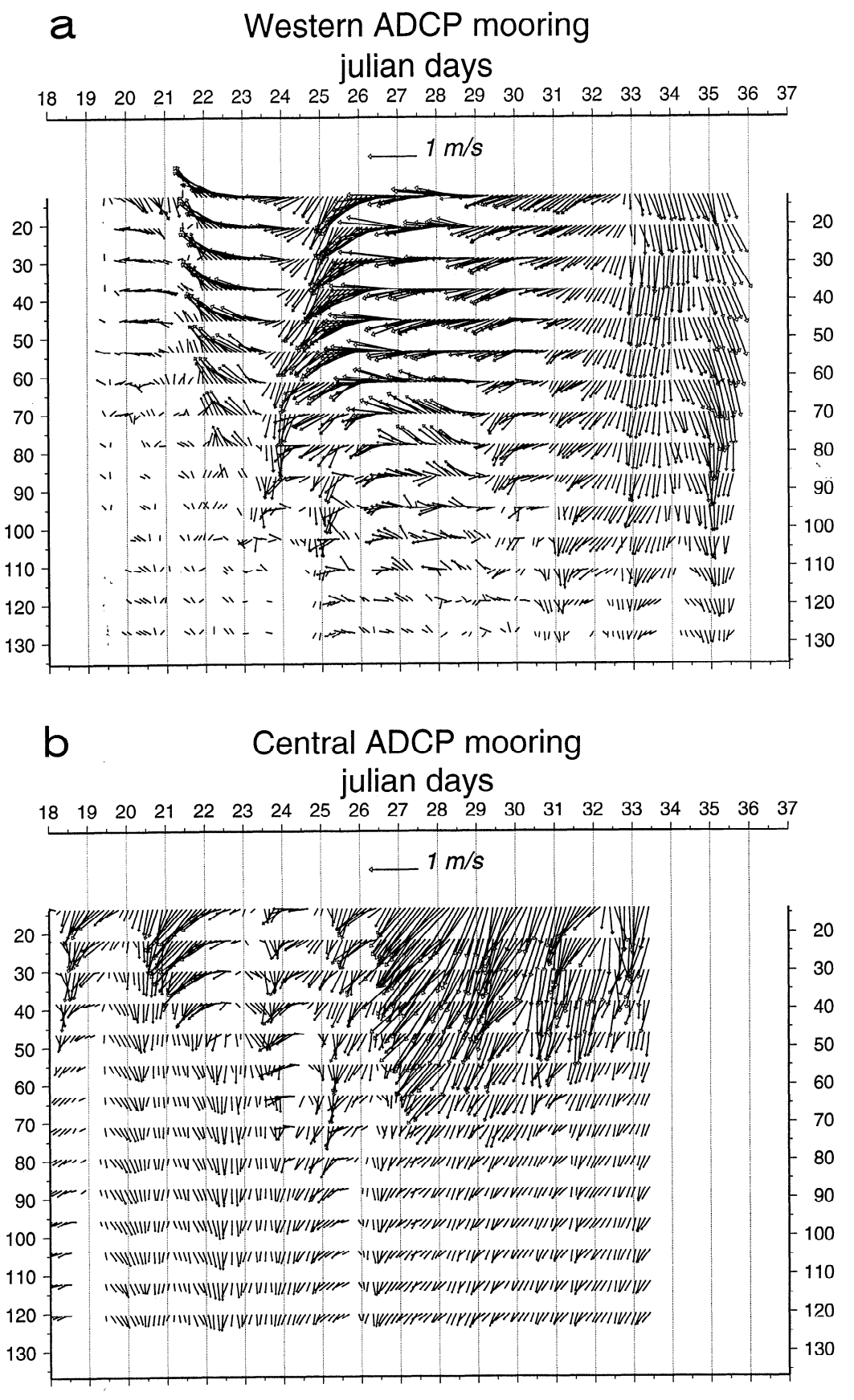

Figure 5. Three-hourly stick diagrams of the currents measured at the deep mooring sites (a) D1 (western), (b) D2 (central), and (c) D3 (eastern) by upward looking ADCPs. A low-pass filter (half power at 40 h) was applied to eliminate high frequency astronomical tide components. Vectors with magnitude less than 0.1 m s^{-1} are not plotted.

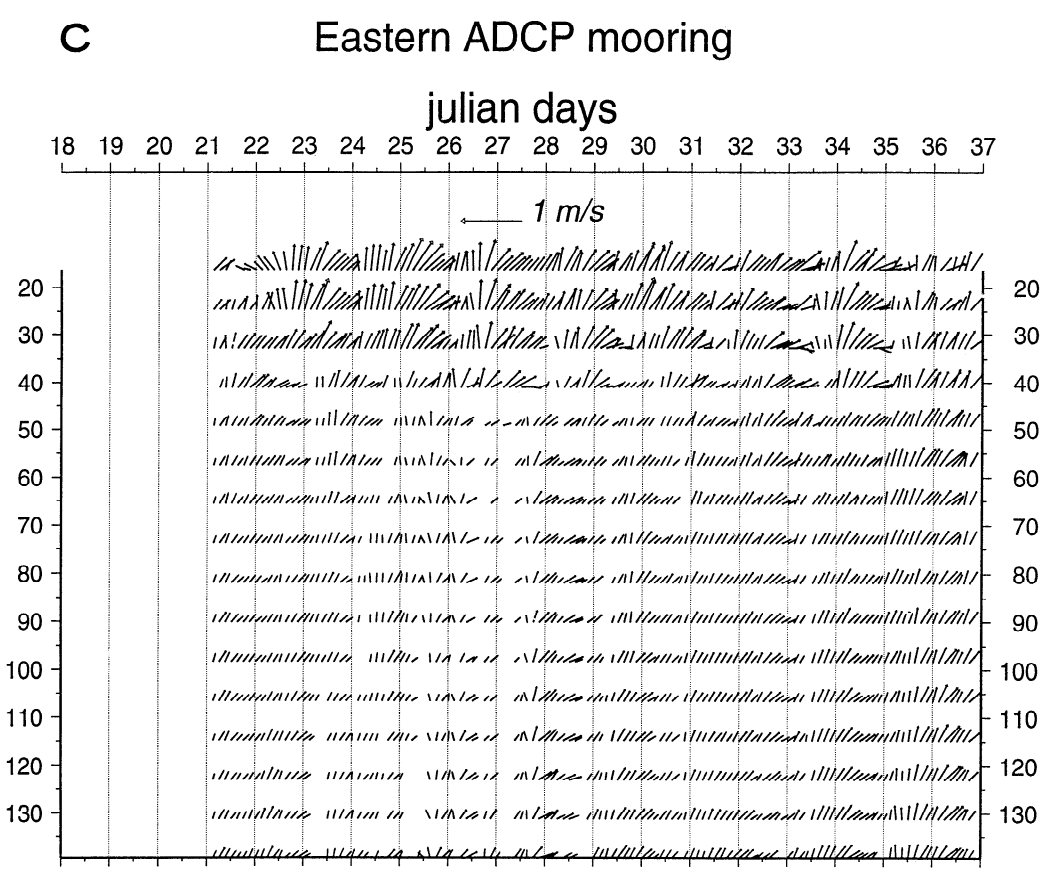

Figure 5. (continued)

throughout the water column. The intensification of the currents after January 24 in the central and western moorings reflect the growing influence of the anticyclonic eddy in the dynamics of this area of the gulf. On February 1, currents at the central site (D2) again reached high values. This is a combination of the effects of the weak wind intensification on that day and renewed southeastward shift of the anticyclonic eddy. In contrast, the steady and vertically coherent current pattern registered in the eastern mooring (D3) toward the end of the observation is consistent with the presence of a large-scale flow with a dominant depth independent behavior.

2.3. Temperature Structure

Two transects along the line of moorings are presented (Plates 2a and 2b). The first is a CTD line carried out from January 18 to 20 (C1), before the event, and the second is a line carried out with Seasoar 2 days after the event, on January 23-24 (S4). The former has an average horizontal resolution of 10 km, and the latter is a more detailed section with a resolution of approximately 3 km.

A number of weak events took place before the start of line C1 (Plate 2a), although during most of the transect the wind speeds were low (maximum of about 10 m s^{-1} but typically 5 m s^{-1}). The shape of the thermocline, depressed in the western gulf and rising toward the surface in the east, forms the "ridge" described in the early surveys [*Blackburn,* 1962].

As described by *Barton et al.* [1993], after the event the thermocline deepens to 100 m in the west (line S4, Plate 2b). An intense horizontal front, also seen in the images, develops west of the axis of the wind, producing the pronounced slope of the isotherms toward the surface. Below the wind axis, intense mixing alters the temperature field down to 60 m depth and produces a lenslike shape in the thermocline. This is a consequence of entrainment and heat exchange between surface and subsurface waters. The minimum surface temperature observed after the event in this section is 17.5°C, about 6°C lower than either the core of the eddy, some 40 km to the west (at about 95.7°W), or the warmest water found in the east. Maximum wind stress curl occurred before the crossing and probably closer to the coast. Nevertheless, this section experienced high wind curl east of 95°W. The thermocline here does not rise toward the surface, as expected from consideration of Ekman divergence such as those illustrated in the model of *Crepon and Richez* [1982]. Instead, it is found to be 5 to 10 m deeper than before the event. The mixed layer is now 25 m deep, on average, and overlays the strongest vertical temperature gradient of this crossing, some 0.8°C m^{-1}. This is consistent with entrainment sharpening the thermocline.

Plate 2c represents the difference between the temperature fields measured after (on January 23-24, Plate 2b) and before the event (from January 18 to 21, Plate 2a). Before January 21 the gulf had already been altered by previous winds, therefore it is not possible to choose a single "reference" profile to measure the effect of the wind on the vertical structure. Instead, smoothed versions of both fields are used to calculate value-by-value differences.

In the western gulf, west of 95.5°W, the occurrence of intense positive anomalies (6 to 8°C warmer) at 80-90 m

depth are caused by pronounced deepening of the thermocline. Above the thermocline the bulk of the water within the eddy shows slightly higher temperatures, consistent with their origin west of the gulf. Below the surface, negative anomalies centered at about 50 m and 95.2°W are produced by the local elevation of the thermal structure.

The central gulf (95.3°W), also shows negative temperature anomalies (Plate 2c) due to intense entrainment processes below the wind jet. The shallow isotherms of the thermocline (Plate 2b), between 18 and 20°C, are elevated, while the deep part of the thermocline, between 16 and 14°C, is depressed and the overall stratification is greatly weakened. The relative cooling and heating observed at levels down to 60 m (Plate 2c), below the original thermocline depth, are the combined result of near-surface vertical wind- and shear-induced mixing.

In the eastern gulf (east of 95°W), where the winds are weaker, vertical mixing is less intense and does not penetrate the thermocline. A band of warming (Plate 2c) is evident near 30 m at the base of the thickened mixed layer, while the near-surface waters are cooler, both changes resulting from the thickening of the surface mixed layer due to entrainment. At the same time, at slightly deeper levels, temperatures are at least 0.5°C cooler than before due to upwelling of cold water. As a result, the interface is strengthened and compressed.

The rapid surface cooling and mixing of the water column beneath the axis of the wind are illustrated in the thermistor chain record (Figure 6a) of the central mooring (site D2 in Figure 2). The outcropping of the 19°C isotherm at the surface coincides with the peak of the event. As the following calculation demonstrates, however, increased evaporative cooling is not sufficient to account for this large and rapid sea surface temperature change (about 6°C in 24 hours). Following the procedure set out by *Gill* [1982], we estimate that the maximum heat loss from the sea surface due to latent heat flux (evaporation), sensible heat flux (direct thermal transfer), and longwave radiation heat loss is 172 W m^{-2}. These conditions occurred at the beginning of the event, when the air temperature was 23.9°C, sea surface temperature was 23.2°C, relative humidity was 85%, and wind speed was 20 m s^{-1}. Assuming that these conditions existed throughout the 48 hours of the event, the maximum decrease in temperature ∂T of the water column at 35 m is

$$\partial T = F t / C_p H \rho \approx 0.21 \text{ °K} \quad (1)$$

where F is heat flux, t is time, C_p is the specific heat capacity of seawater (4×10^3 J kg^{-1} K^{-1}), H is depth of the water column, and ρ the density of sea water (1024 kg m^{-3}). The relative humidity dropped as low as 55% during the event, but by this time the (air-sea surface) temperature difference was 7.5°C and the sensible heat flux was comparable in magnitude and opposite in sign to the latent heat flux, with the total heat loss being 15 W m^{-2}. The above estimate takes no account of solar radiation which is 500 W m^{-2} during full daylight hours and may even alter the sense of ∂T.

The thermistor chain (Figure 6b) at the eastern mooring (site D3 in Figure 2) shows that during the event, from January 21 to 23, the depth of the mixed layer grows by about 10 m to 45 m depth, on average, and the sharpness of the thermocline increases dramatically. The temperature distribution starts to relax after January 25, following the end of the wind event. A secondary thermocline develops near the surface, with maximum temperatures at the uppermost thermistor over 25°C, which reflect hydrographic conditions eastward and farther offshore of the gulf. From January 25 on the thermocline becomes increasingly diffuse; the weak wind events of January 28 and 31 have no significant effect at this mooring.

In summary, the observations at the central mooring are consistent with entrainment below the wind jet being the primary cause of the observed surface cooling. The strengthening of the thermocline east of the wind jet is caused by the thickening of the mixed layer due to entrainment and upwelling from beneath due to Ekman pumping. Both the current and temperature fields show a strong relation between the vertical extent of the currents and the thickness of the mixed layer. Maximum vertical extent is found west of the wind jet, where the thermocline is always deeper. In the central gulf, where the wind is strongest but the thermocline is shallow, the currents extend down to 40 or 50 m depth, reaching greater depths only during the eastward expansion of the eddy after January 27. In the eastern gulf the currents are also strongest in the mixed layer above a strong and shallow thermocline.

2.4. Static and Dynamic Stability

Vertical mixing in stratified conditions depends on both the vertical shear of the mean horizontal currents and on the strength of the vertical density gradients. Once a vertical shear exists, turbulence will extract energy from the mean horizontal motion, but it will only be capable of breaking through a density discontinuity after overcoming the buoyancy force. The gradient Richardson number provides an appropriate criterion for judging whether or not turbulence is strong enough to overcome the static buoyancy of the fluid and deepen the mixed layer. This dimensionless quantity is the ratio of the stability (or Brunt-Väisälä) frequency to the vertical shear,

$$R_i = \frac{N^2}{(\partial_z \mathbf{U})^2} \quad (2)$$

where N^2 is the stability frequency and $\mathbf{U}$ is the horizontal velocity vector. It has been determined that when R_i is larger than 0.25 [*Miles*, 1961; *Howard*, 1961], turbulence cannot be generated by a vertical gradient of velocity.

In order to estimate the gradient Richardson number, time series of current velocity from the upward looking ADCPs and temperature series from the thermistor chains at the central and eastern moorings (D2 and D3) are used. Although there is no thermistor chain record for the western gulf, the distribution of the vertical shear at this site is included for completeness. The calculations of vertical shear (Figure 7), given the vertical sampling of the currents (4 m), have a resolution of $O(10$ m). The calculations of the stability frequency (Figure 8), given the spacing of the thermistors (7.5 m), also have a vertical resolution $O(10$ m). To compute the stability frequency, a piecewise linear fit between temperature and salinity, using simultaneous CTD data, was performed. The Richardson number was calculated by first gridding the data with the method of continuous curvature splines in tension [*Smith and Wessel*, 1990].

The distribution of vertical shear reveals that in the western gulf (Figure 7a), not only do the currents penetrate deeper, but also that it is here that the flow presents least vertical shear

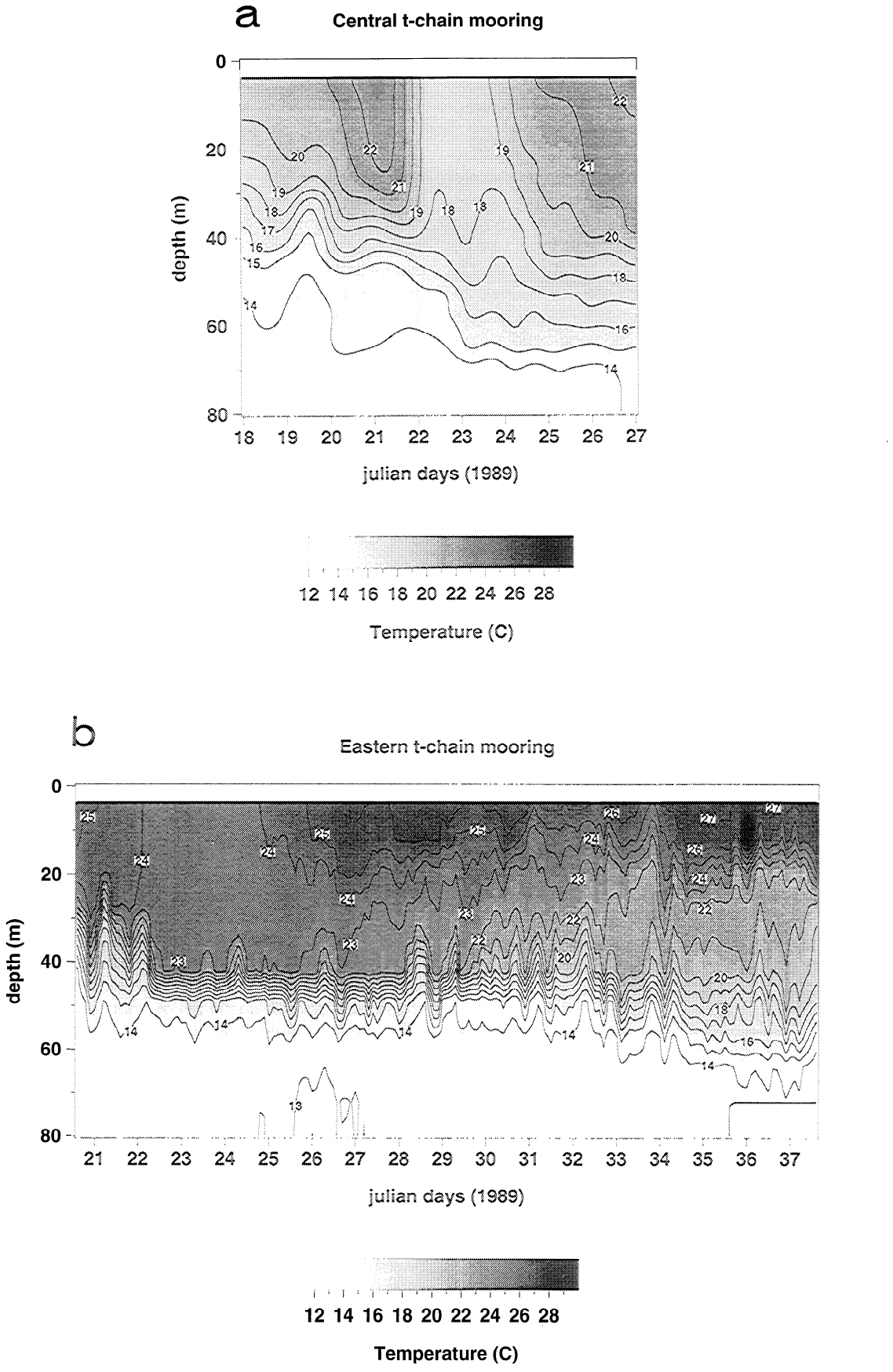

Figure 6. (a) Temperature contours from the thermistor chain (t-chain) record at mooring site D2 in the central Gulf of Tehuantepec. (b) Temperature contours from the t-chain record at mooring site D3 in the eastern gulf.

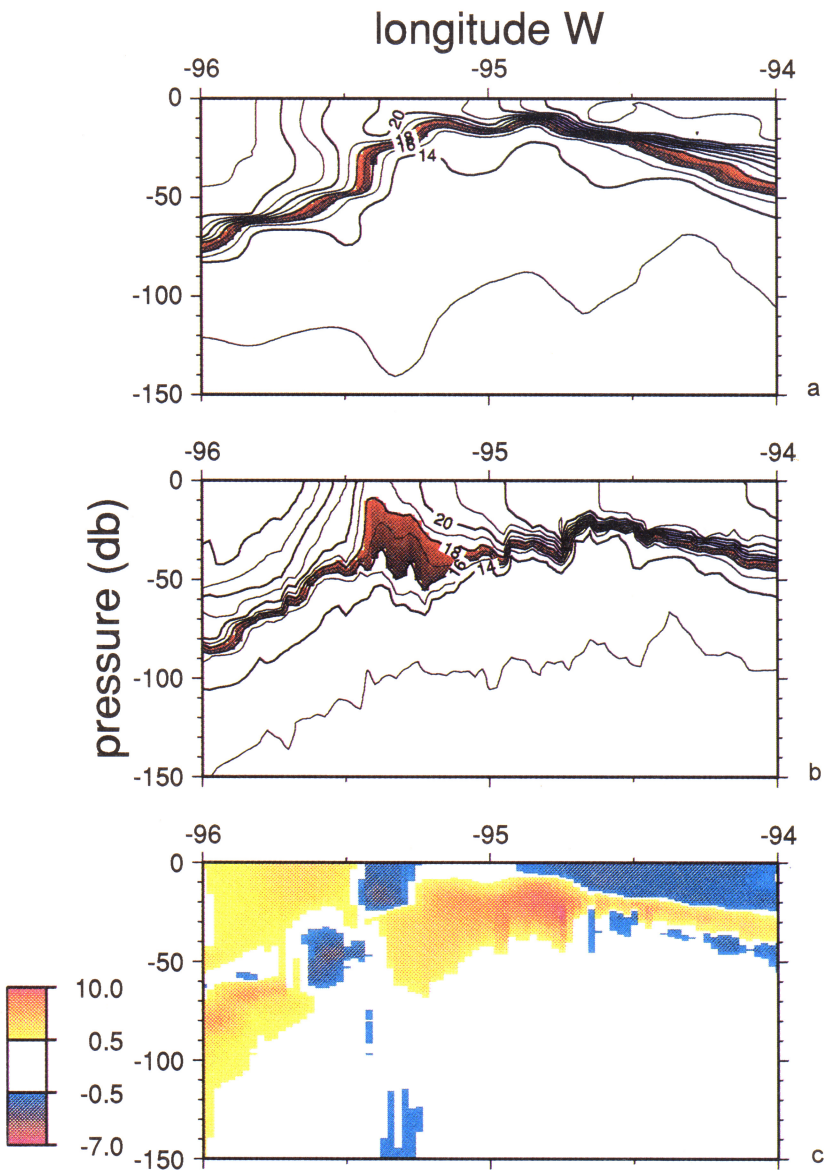

Plate 2. Temperature sections before and after the wind event. (a) Section from a conductivity-temperature-depth probe (CTD) along the mooring line (line C1, from January 18 to 20). (b) Section from a towed CTD system (Seasoar) along the mooring line (line S4, from January 23 to 24). (c) Difference between the temperature fields measured after and before the wind event (S4-C1). Positive differences indicate warmer temperatures after the event.

throughout the whole period of observations. Maximum values are found in the central gulf (Figure 7b) during the most intense phase of the wind event. High shear is also found in the eastern gulf during the event but restricted to the upper 20 m (Figure 7c). Here the maxima coincide with the intensification of the surface flow at a near-inertial period. By comparing the estimates of shear at the three sites it is clear that the shallower maxima are located where the thermocline is nearest to the surface, i.e., below the wind jet and to the east.

The evolution of stability frequency (Figure 8) at the central (D2) and eastern (D3) mooring sites reveals strong changes in stratification. During the most intense phase of the event, on January 21, the mixed layer at the central gulf (Figure 8a) deepens almost immediately. This deepening results from shear-induced entrainment within the offshore current jet, as confirmed by the estimates of the Richardson number (Figure 9a). From January 22 to 25 (Figure 8a) the stability maximum weakens at the same time that the offshore current jet reaches depths below the original thermocline (see Figure 5b). However, the values estimated for the Richardson number (Figure 9a) for January 22 to 25 do not indicate the existence of a turbulent regime below 40 m, meaning that the local vertical shear was not intense enough to overcome the stability of the fluid below the original thermocline depth. This feature occurs due to the advection within the offshore current jet of a cooler and deeper mixed layer produced by wind-stirring earlier in the event and closer to the coast. This result is supported by the satellite image of January 21 (Plate 1a) and others on succeeding days. The coldest part of the temperature anomaly, formed initially to the north of D2, was advected through the mooring and offshore.

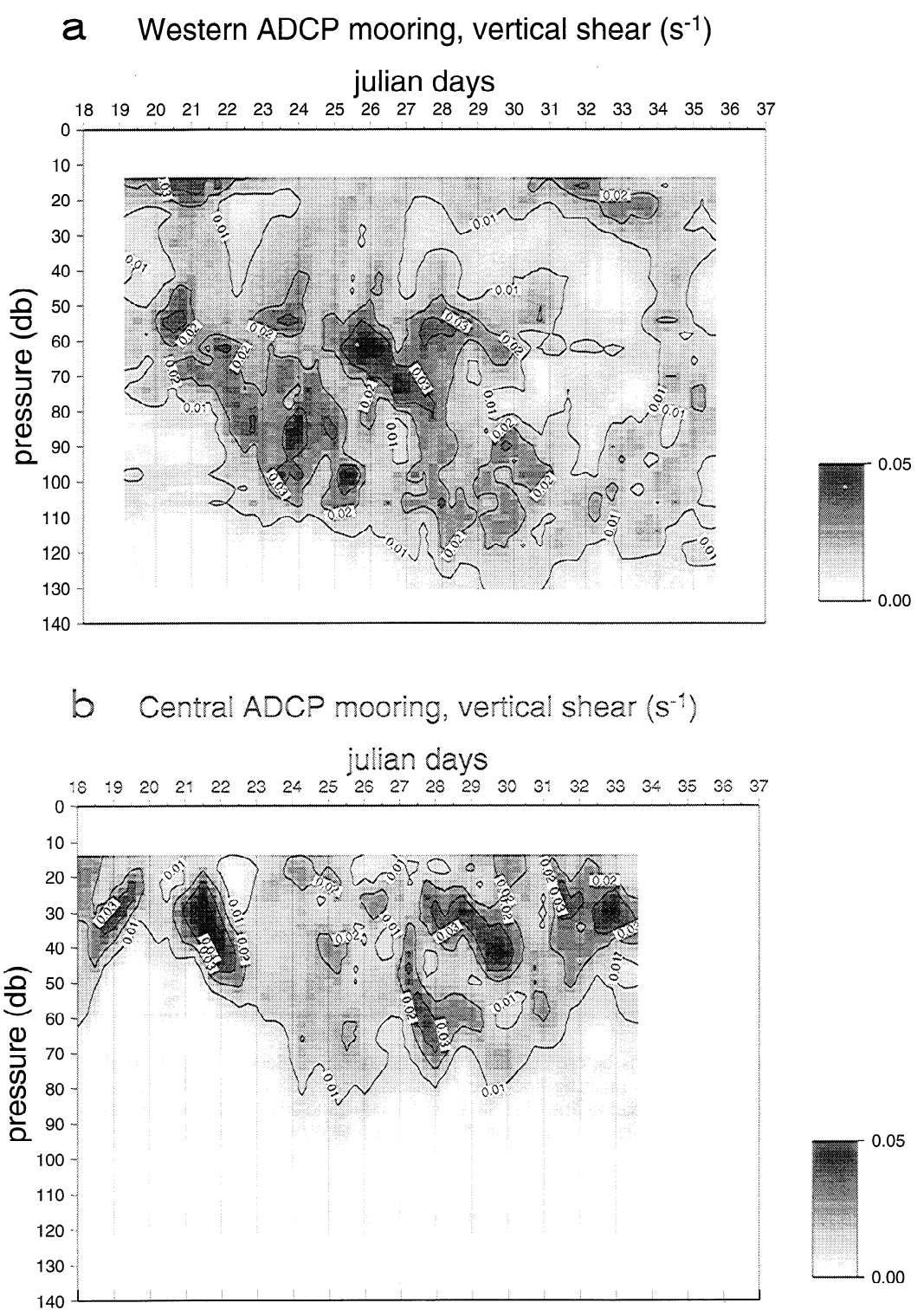

Figure 7. Vertical shear (s^{-1}) from upward looking ADCP data for moorings (a) D1 (western), (b) D2 (central), and (c) D3 (eastern).

At the eastern mooring site (Figure 8b) the mixed layer during the event responds with a similar, if slightly less pronounced, deepening of the mixed layer. Afterward, however (from January 24 onward), stratification continues to increase and creates a strong boundary to the vertical penetration of the currents. Although the Richardson number reaches minimum values (Figure 9b), which are indicative of highly turbulent flow, these are restricted to the mixed layer by the increasing stability of the interface and do not reach the underlying fluid.

3. Summary and Discussion

The climatic mean thermocline is very shallow (50 m) in this region of the eastern tropical Pacific. This property

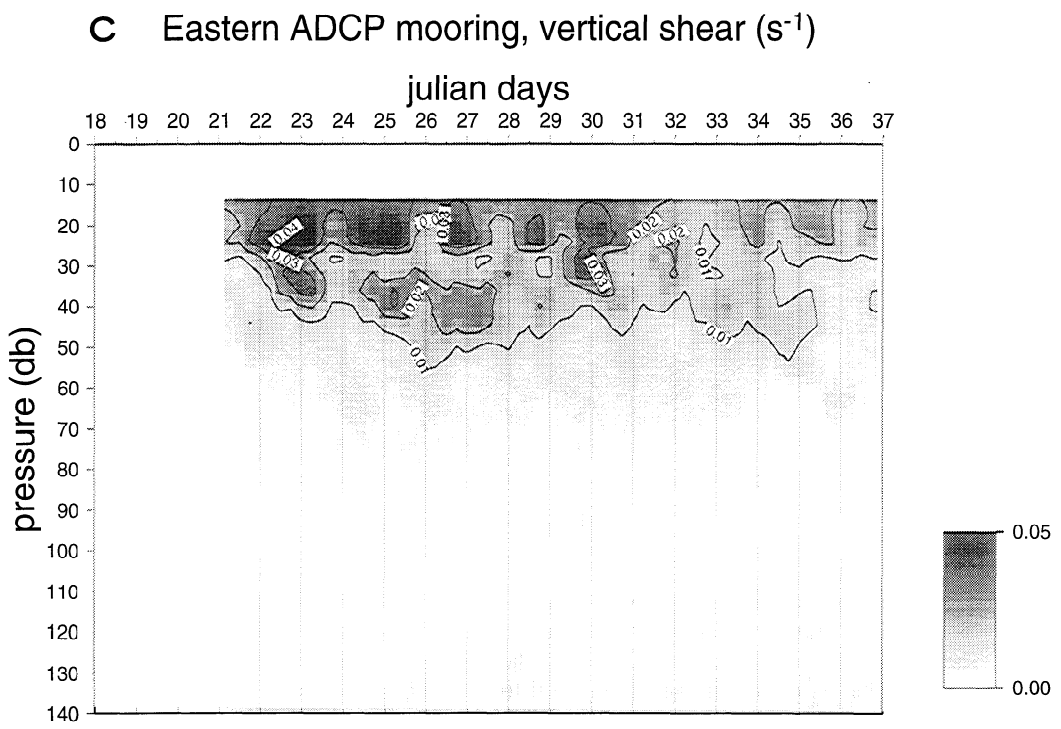

Figure 7. (continued)

implies that Ekman convergence and divergence will have quite different effects; in a region of Ekman convergence, adiabatic deepening of the thermocline is essentially unlimited, and in a region of divergence, its shallowing is hindered by the proximity of the surface. These differences are evident in the patterns of vertical mixing (as measured by high values of vertical shear) across the Gulf of Tehuantepec. In the western gulf, where there is Ekman convergence, vertical mixing extends down to a maximum of 120 m, whereas in the eastern gulf, where there is divergence, it is restricted to a shallow surface layer and the upper part of the thermocline. In the latter region, entrainment due to wind stirring, coupled with Ekman divergence, acts to sharpen the vertical density gradient at the base of the mixed layer. The entrainment also inhibits the development of strong, near-surface density gradients and hence weakens the near-surface geostrophic flow field. As a consequence, the observed circulation differs from that indicated by considerations of Ekman pumping alone. Specifically, a strong anticyclonic eddy develops in the western gulf, but there is no corresponding cyclone in the eastern gulf.

The circulation following a wind event is largely restricted to the upper layer above the thermocline. At the onset of the event this layer is already shallower in the eastern gulf. The mixed layer is thicker in the western gulf, the circulation is more vigorous, and it reaches deeper in the water column. Most of the water incorporated into the eddy comes from the west, outside the gulf.

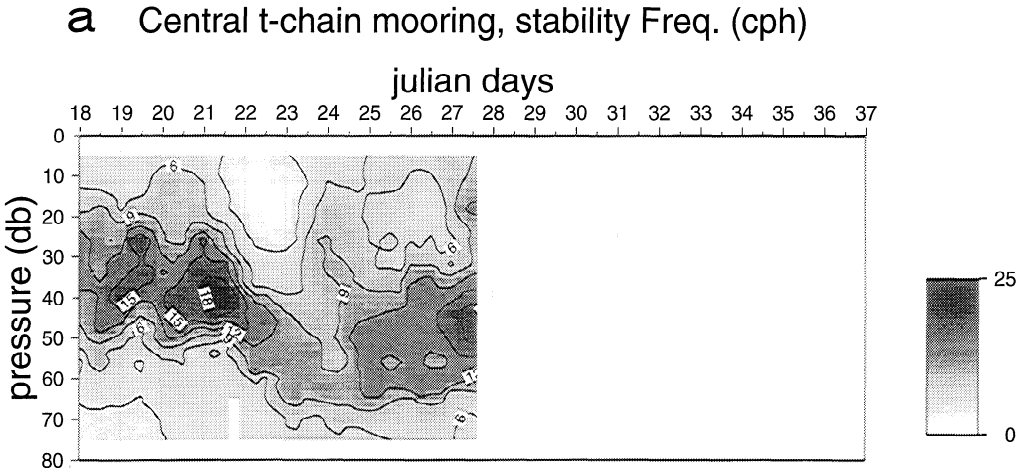

Figure 8. Stability frequency in cycles per hour (cph) from thermistor chain (t-chain) data for (a) D2 (central) ADCP mooring and (b) D3 (eastern) ADCP mooring.

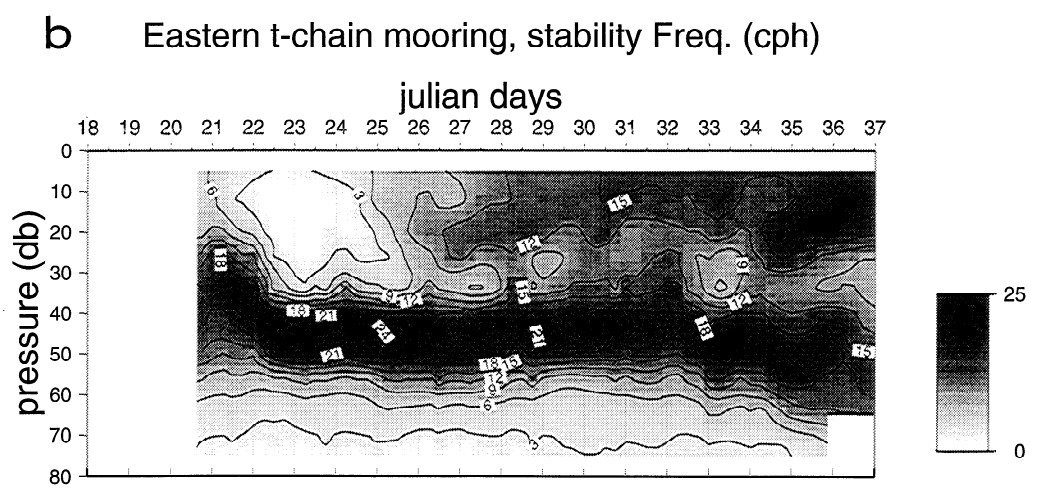

Figure 8. (continued)

Upwelling of the thermocline due to Ekman pumping is not the main cause of the drastic lowering of sea surface temperatures. The intersection of the thermocline with the surface should occur in the region of maximum wind curl to the left of the axis of the wind in the eastern gulf. The image of January 21, however, shows that the lowest temperatures are not in the eastern but in the central gulf, beneath the axis of the wind. Furthermore, although the alteration of the vertical structure was observed after maximum wind curl occurred, the thermocline deepens throughout the gulf; it does not rise toward the surface in the eastern gulf. Entrainment induced by vertical shear in the offshore jet penetrates deeper than elsewhere, producing vertical mixing and the intense temperature minimum observed in the central gulf.

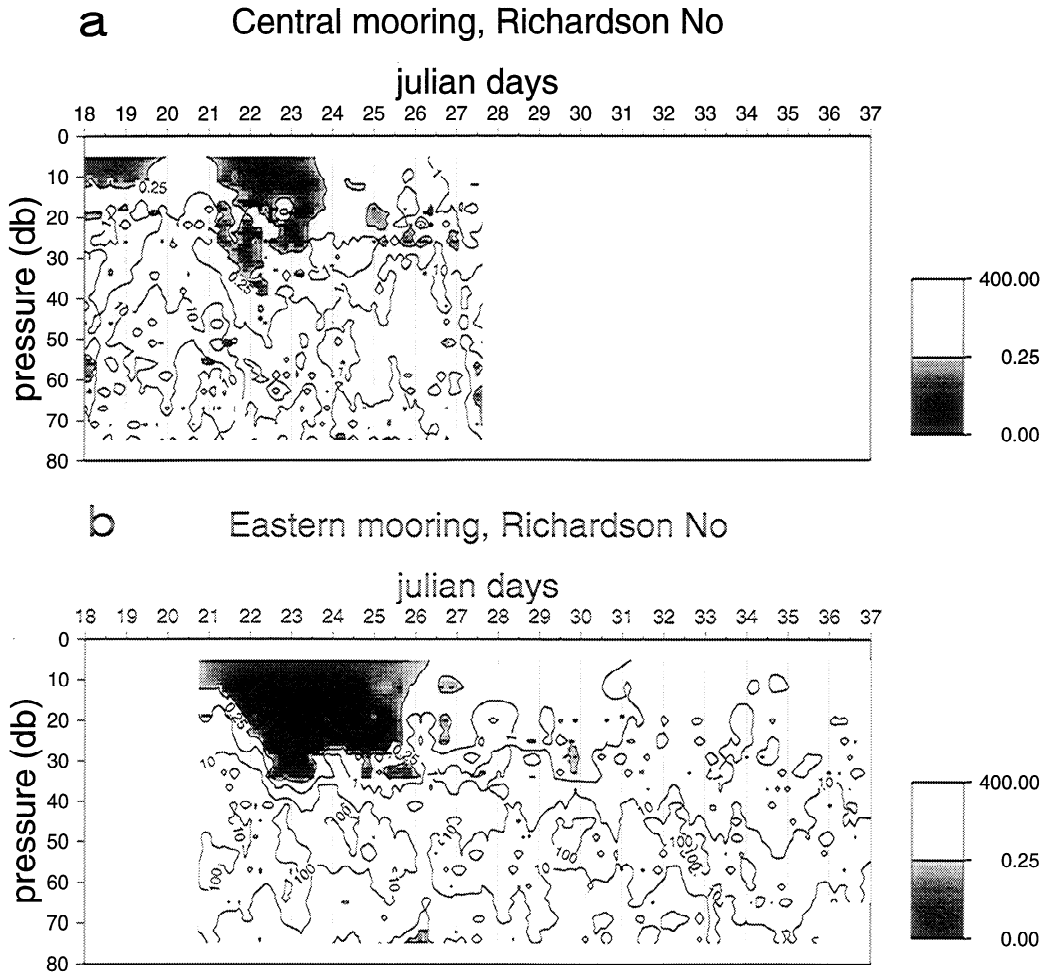

Figure 9. Richardson number from t-chain and ADCP data for (a) D2 (central) ADCP mooring and (b) D3 (eastern) ADCP mooring.

In the eastern gulf, entrainment lowers the surface temperature to a lesser extent than in the central gulf by mixing the upper thermocline and deepening the mixed layer. This, combined with the elevation of the vertical structure by Ekman pumping, decreases the temperature contrast between layers while intensifying the thermocline. The critical factor which restricts both the vertical penetration and the strength of the surface flow is the maintenance of the mixed layer during a wind event. *Wyrtki* [1964] describes a similar situation in the Costa Rica Dome. In this case the thermocline remains stationary because the upwelling of cool water is compensated by the downward turbulent flow of heat from the mixed layer.

The models described in the introduction are now discussed. After *Clarke*'s [1988] results it is clear that any asymmetry in the forcing will be reflected on the circulation. An average wind speed of 10 m s^{-1} corresponds to an inertial radius for the wind of around 260 km. The associated negative wind curl would tend to strengthen the anticyclonic circulation and weaken the cyclonic circulation east of the jet. There are some indications that the axis of the wind jet does curve to the right far from the coast, but the inertial radius of the wind is twice the observed radius of the anticyclonic eddy. Furthermore, the forcing appears to be mostly symmetrical around the eddy generation area, therefore the eddy scale does not seem to be directly linked to the inertial scale of the forcing. Another feature of that model is the production of symmetrical pycnocline elevation and depression, east and west, respectively, of the wind jet, whereas the observations indicate a much stronger depression.

McCreary et al.'s [1989] model provides quite a good representation of the observed situation. This model includes entrainment which weakens the cyclonic eddy and horizontal advection which produces realistic "wrapping around" of warm and cold tongues, as seen in the sea surface temperature images on the circumference of the eddy. The model is limited, however, in that its parameterization of entrainment depends only on the pycnocline elevation above its unperturbed depth (50 m), not on the strength of the surface wind, as is the case in reality. In the observations the thermocline in the central gulf under the wind axis is much deeper at the height of the event and surface temperatures attain their minimum values there. In the model, coldest surface temperatures are produced not where the wind is strongest but where the pycnocline is most elevated. The model pycnocline is not elevated beneath the wind maximum because this is the position of zero wind stress curl, and hence the model cannot reproduce the observed mixing and cooling there.

Acknowledgments. This project was supported financially by the Consejo Nacional de Ciencia y Tecnologia (Mexico), the Natural Environment Research Council (United Kingdom, grant GR3/6719) and by the U.S. Office of Naval Research (contract N00014-90-J-1177). The British Council facilitated funds for liaison between the United Kingdom and Mexico (grant 922/37). The first author also wants to acknowledge the support of the Overseas Research Scheme (United Kingdom). We would like to thank our colleagues on both ships who provided support essential to carry out the field work. Part of the current meter data was kindly provided by the Grupo Tehuantepec (CICESE, Oceanografía Física; J.M. Robles, M. Lavin, M.L. Argote, and J. García). Thanks are due to Jeff Hawkins of NORDA, Stennis Space Center, Mississippi, who preprocessed the AVHRR imagery and forwarded analyses to the ships, and to Dave Enfield, Hurricane Research Center, Miami, Florida, who provided daily weather forecasts for us at sea and contributed to the scientific discussions. Also, I wish to thank Ma. Luisa Argote and Miguel Lavin, both at the Department of Physical Oceanography of CICESE, as well as J. P. McCreary and an anonymous reviewer, for their helpful comments.

References

Barton, E.D., M.L. Argote, J. Brown, P.M. Kosro, M. Lavin, J.M. Robles, R.L. Smith, A. Trasvina, and H.S. Velez, Supersquirt: Dynamics of the Gulf of Tehuantepec, Mexico, *Oceanography*, *6*(1), 23-30, 1993.

Blackburn, M., An oceanographic study of the Gulf of Tehuantepec, *Spec. Sci. Rep. 404*, U.S. Fish and Wildlife Serv., Washington, D. C., 1962.

Brandhorst, W., Thermocline topography, zooplankton standing crop, and mechanisms of fertilization in the eastern tropical Pacific. *J. Cons. Cons. Int. Explor. Mer*, *24*(1), 16-31, 1958.

Brown, J., E.D. Barton, A. Trasvina, H.S. Velez, M. Kosro, and R.L. Smith, Estimation of surface winds from upward looking acoustic Doppler current profilers, *J. Geophys. Res.*, *97*(C11), 17,925-17,930, 1992.

Clarke, A. J., Inertial wind path and sea surface temperature patterns near the Gulf of Tehuantepec and Gulf of Papagayo, *J. of Geophys. Res.*, *93*(C12), 15,491-15,501, 1988.

Crepon, M., and C. Richez, Transient upwelling generated by two-dimensional atmospheric forcing and variability in the coastline, *J. Phys. Oceanogr.*, *12*, 1437-1457, 1982.

Christensen, N., V. R. De la Paz, and V. G. Gutiérrez V. G., A study of sub-inertial waves off the west coast of Mexico, *Deep Sea Res.*, *Part* A, *30*(8A), 835-850, 1983.

Enfield, D.B., and J.S. Allen, The generation and propagation of sea level variability along the Pacific Coast of Mexico, *J. Phys. Oceanog.*, *13*, 1013-1033, 1983.

Gill, A. E., *Atmosphere-Ocean Dynamics*, Inter. Geophys. Ser., Vol. 30, Academic, San Diego, Calif., 1982.

Howard, L.N., Note on a paper of John W. Miles, *J. Fluid Mech.*, *10*, 509-512, 1961.

Leben, R.R., J.D. Hawkins, H.E. Hurlburt, and J.D. Thompson, Wind driven anticyclonic eddies in the eastern Pacific (abstract), *Eos Trans AGU*, *71*(43), 1364, 1990.

McCreary, J. P., H. S. Lee, and D. B. Enfield, The response of the coastal ocean to strong offshore winds: with application to circulation in the Gulfs of Tehuantepec and Papagayo, *J. Mar. Res.*, *47*, 81-109, 1989.

Miles, J. W., On the stability of heterogeneous shear flows. *J.Fluid Mech.*, *10*, 496-508, 1961.

Smith, W.H.F., and P. Wessel, Gridding with continuous curvature splines in tension, *Geophysics*, *55*(3), 293-305, 1990.

Strong, A. E., R. J. De Rycke, and H. G. Stumpf , Satellite detection of upwelling and cold water eddies, paper presented at 8th International Symposium on Remote Sensing of the Environment. Environ. Res. Inst. of Mich., Ann Arbor, 1067-1081, 1972.

Stumpf, H. G., Satellite detection of upwelling in the Gulf of Tehuantepec, Mexico, *J. Phys. Oceanogr.*, *5*, 383-388, 1975.

Stumpf, H. G., and R. V. Legeckis, Satellite observations of mesoscale eddy dynamics in the eastern tropical Pacific Ocean, *J. Phys. Oceanogr.*, *7*, 648-658, 1977.

Wyrtki, K., Upwelling in the Costa Rica Dome, *Fish. Bull.*, *63*(2), 355-372, 1964.

E. D. Barton and H.S. Velez, School of Ocean Sciences, University of Wales, Menai Bridge, Gwynedd, LL59 5EY, Wales, United Kingdom.

J. Brown, Fisheries Laboratories, MAFF, Lowestoft, Suffolk, NR33 0HT, England, United Kingdom.

P. M. Kosro and R. L. Smith, College of Oceanography, Oregon State Universitry, Corvallis, OR, 97331.

A. Trasviña, Departamento de Oceanografía Física, CICESE, Ap. Postal 2732, Ensenada, Baja California, 22800, México. (email: trasvi@cicese.mx)

(Received December 6, 1993; revised March 9, 1995;
accepted April 19, 1995.)